Appl. Phys. B 43, 127–138 (1987)

Applied Physics B Photophysics and Laser Chemistry

Operational Characteristics of a MAGPIE Coaxial CO_2 Discharge System

V.A. Seguin, H.J.J. Seguin, C.E. Capjack, and S.K. Nikumb

Department of Electrical Engineering, The University of Alberta, Edmonton, Alberta, T6G 2G7 Canada

Received 6 May 1986/Accepted 24 November 1986

Abstract. The operational characteristics of a convectively cooled Magnetically stabilized, Photo-initiated, Impulse-enhanced, Electrically-excited (MAGPIE) coaxial discharge system are described. Terminal behavior is examined as a function of several parameters, such as gas flow, pulser ionization, and magnetic field strength. In-situ plasma potential measurements are also presented, which indicate that CO_2 attachment effects have considerable influence on the spatial electrical characteristics of the gas discharge.

PACS: 42:55 Dk

Magnetic fields have been found to be useful in a number of gas laser applications. These have included position stabilization of the plasmam column in convective flow lasers [1–3]; as well as the generation of gas circulation in a CO_2 laser, without the need of a mechanical blower [4]. Experimental research has also demonstrated that crossed electric and magnetic fields may effectively suppress electro-thermal instabilities in a CO_2 laser plasma. This magnetic stabilization approach was originally demonstrated in a small-scale experiment using a conventional transverse discharge configuration [5, 6].

In addition, several researchers have suggested the use of a coaxial electrode geometry as an alternative to the usual axial or transverse designs [7–10]. This would consist of two cylindrical electrodes, one inside the other, enclosing an annular gain volume. Recently, the magnetic discharge stabilization approach has been extended to just such a coaxial electrode configuration [11, 12].

The operating principle behind the magnetically stabilized coaxial discharge system may be observed in the schematic of Fig. 1. Two cylindrical electrode elements are assembled, one inside the other. A radial electric field E_r, and current density J_r, are established between the two concentric electrodes. In addition, an axial magnetic field B_z is applied to the discharge by an external solenoid. The resulting Lorentz $J_r \times B_z$ force generates a rapid rotational motion of the charge species within the discharge volume, with a concomitant Hall current component J_θ.

This vigorous electron and ion transport, particularly in the space-charge regions near the electrode surfaces, helps to suppress the formation of electro-thermal instabilities. In addition, momentum is

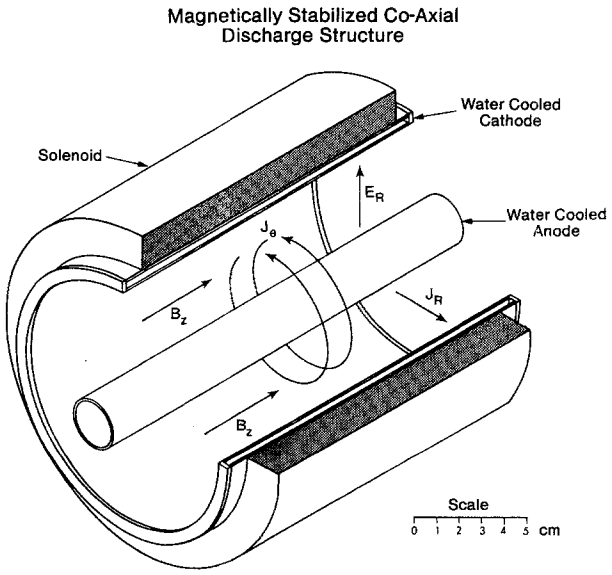

Fig. 1. Magnetically stabilized coaxial discharge system

coupled from the charged species to neutral molecules through collisions. Thus, a significant bulk rotational motion of the plasma is also observed.

More recently, a large volume coaxial discharge system has been developed and tested [13], for eventual CO_2 laser applications. This device utilized a multi-element, fluid-ballasted cylindrical cathode as the central electrode element [14]. Also, non-self-sustained operation was obtained with a pulser pre-ionization system. The complete system, referred to as the MAGPIE device, exhibited excellent discharge stability, at power densities of up to 5 kW/l. However, the magnetically-induced plasma motion was unable to cool the discharge to temperatures low enough to permit efficient laser operation.

1. MAGPIE Gas Transport System Development

As a result of these considerations, a new MAGPIE coaxial discharge system was developed, which incorporated a mechanical blower for convective cooling of the plasma. This device is depicted schematically in Fig. 2. A simple cylindrical tank served as the vacuum enclosure, with O-ring-sealed doors at each end. The electrode system consisted of a multi-element cathode mounted along the system axis, surrounded by a helical coil of copper tubing, which served as the outer grounded anode. In addition, the axial magnetic field required for operation was generated by passing a large dc current through this same coil; which thereby also acted as an electromagnetic solenoid. The active discharge region was 40 cm long, with a 6 cm electrode separation, and an enclosed volume of 10 l.

In order to provide convective gas cooling, an axial flow geometry was selected. As illustrated in Fig. 2, an axial flow fan was installed at each end of the electrode assembly. Together these blowers circulated the laser gas mixture through the annular discharge region, then through a spiral-wound heat exchanger, and finally back along an outer annular flow return duct. This unusual flow geometry permitted a high gas flow rate in a device of comparatively small physical size.

The excitation system for this system was based on the PIE (Photo-initiated, Impulse-enhanced, Electrically-excited) process [15, 16]. A high repitition rate thyratron pulser, illustrated schematically in Fig. 3, was used to generate electrical impulses of about 100 ns duration and up to 10 kV in amplitude. The repetition rate was fixed for these experiments at 5 kHz, but the average pulser power could be continuously varied up to about 2 kW. When coupled to the electrodes, this pulser provided a uniform background photo-impulse-ionized plasma, which was then subsequently pumped by a much larger but nonavalanching dc power supply.

Due to speed limitations of the axial flow fans, the maximum gas flow velocity for these experiments was about 50 m/s. Consequently, only about 12 kW of dc pumping power could be deposited into the discharge while maintaining a sufficiently low gas temperature for efficient vibrational excitation. Given the very large discharge volume in this device, the operating power density was thus only about 1.2 kW/l. Although this value is lower than reported for several other CO_2 laser systems [17, 18], it is anticipated that the useful power loading of the machine could be increased substantially by improving the performance of the blower system.

2. Discharge Terminal Characteristics

Several V–I curves were obtained for the MAGPIE gas transport discharge system, each with a different variable parameter. First, the terminal behavior was

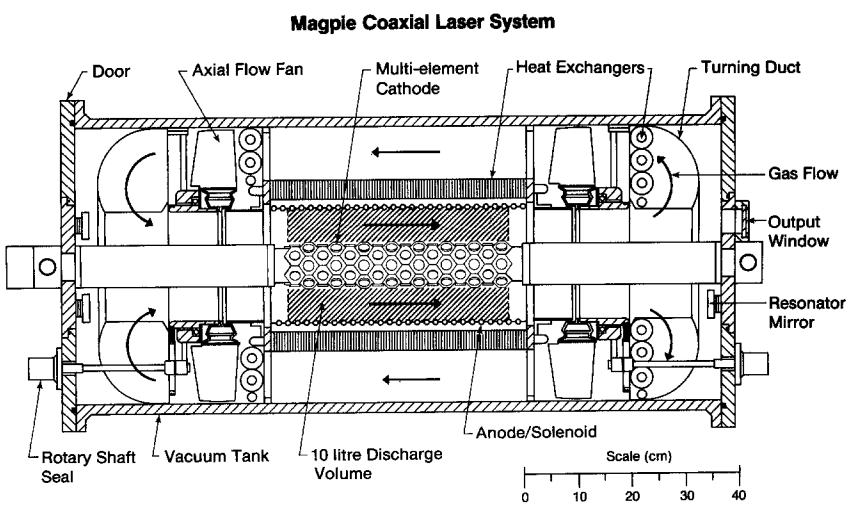

Fig. 2. MAGPIE coaxial gas transport laser system

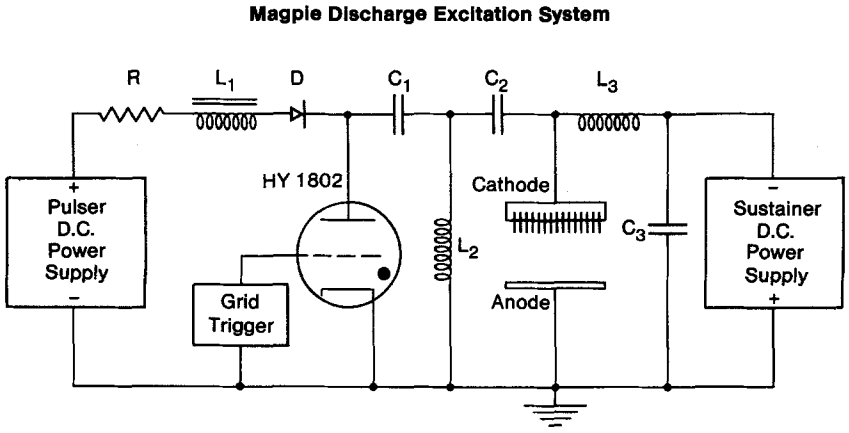

R = Ballast Resistor = 1KΩ
L_1 = Saturable Inductor = 1000 – 20 mH.
D = Charging Diode = 20 kV. P.I.V.
C_1 = Storage Capacitor = 4nF.
L_2 = Recharge Inductor = 240 μH
C_2 = Coupling Capacitor = 10 nF.
L_3 = R.F. Choke = 100 μH.
C_3 = Filter Capacitor = 10 nF.

Fig. 3. MAGPIE electrical excitation system

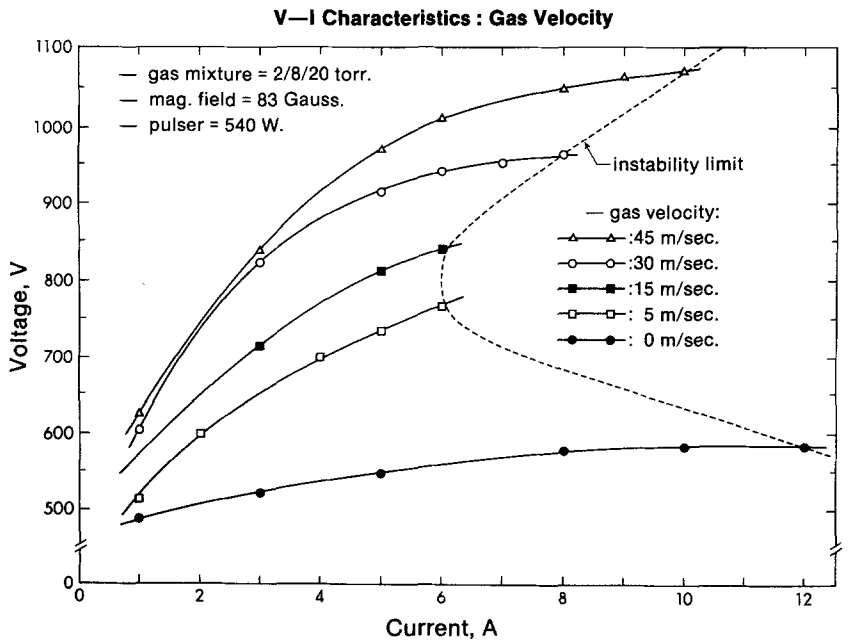

Fig. 4. V–I characteristic: gas velocity

examined as the gas flow was varied. Here the discharge operating voltage, for a given current, was observed to increase substantially as the gas flow was increased. This effect is illustrated in Fig. 4. The marked increase in plasma impedance was attributed to the decreased conductivity of the plasma as the gas temperature was reduced. Thus, the terminal characteristics immediately indicated that the gas transport system was having the desired effect of cooling the discharge. Also shown in this plot is the instability threshold; which is seen to increase in terms of both voltage and current as the gas flow is increased.

In order to examine the effect of gas flow on plasma stability, the maximum stable input power (neglecting ballast resistance losses) is plotted as a function of gas velocity in Fig. 5. As expected, the instability point is seen to increase almost linearly as the gas flow is raised, for flow velocities above 10 m/s. However, as the flow velocity is reduced below this value to zero, the maximum input power again rises markedly.

This stable low-flow regime of operation is also apparent through visual observation of the discharge. Without gas flow, the plasma is seen to be very stable and uniform. As the blower speed is slowly increased,

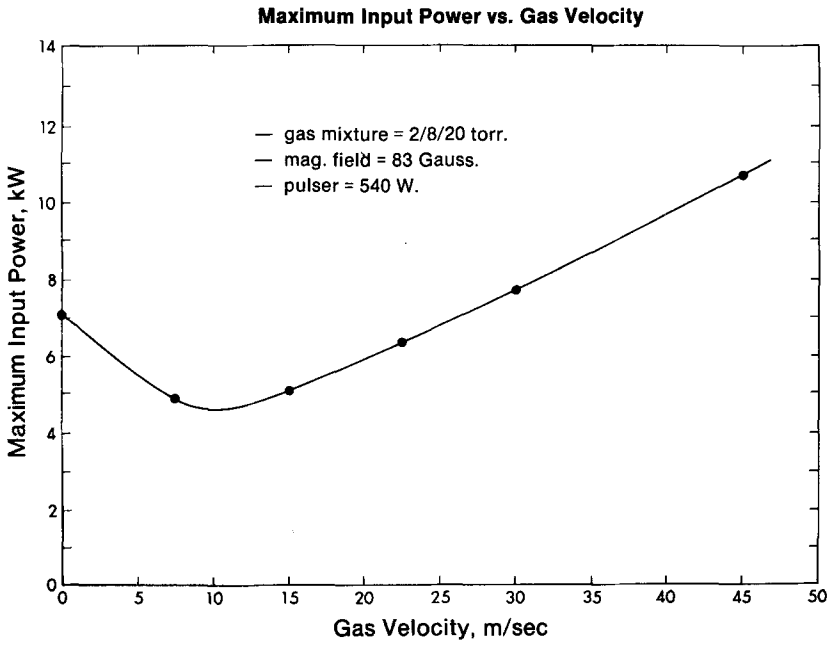

Fig. 5. Maximum input power vs. gas velocity

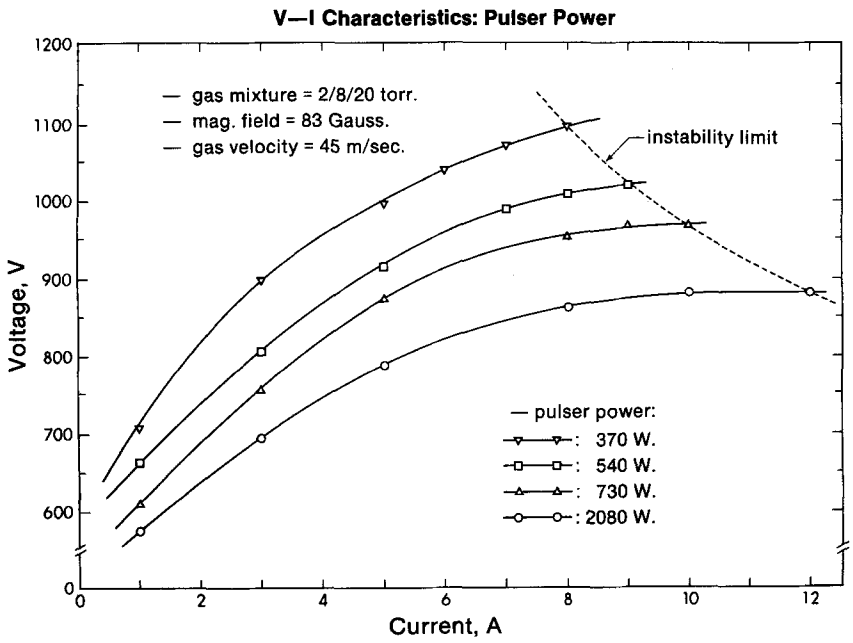

Fig. 6. V–I characteristic: pulser power

the discharge is first seen to oscillate axially, becoming very non-uniform. At this point, instabilities are seen to occur at relatively low current levels. As the gas velocity increases still further, the discharge again becomes progressively more uniform and stable, even as the input power increases.

The plasma stability phenomena described above may possibly be due to a transition between stabilization mechanisms. It has been documented that the gas temperature is very high (>600 K) when external gas flow is absent [13]. Under these conditions, the gas density is lower than it is with convective cooling. Consequently, the plasma is less collision-dominated, and the magnetic field has a much greater influence on the behavior of the charged species. The result is enhanced discharge stability.

However, when external gas flow is introduced, the gas temperature decreases markedly. This has the effect of increasing the gas density, which in turn reduces the effectiveness of the magnetic field. Consequently, discharge stability is observed to decrease. From this point onward, the increasing gas flow rate progressively reduces the residence time of the gas within the discharge region. This effect allows an

increasing power density to be achieved within the discharge before instabilities occur [19].

The influence of pulser preionization on terminal characteristics is depicted in Fig. 6. Increasing the pulser power was found to greatly decrease the plasma impedance. During data collection in Fig. 6, it was observed that full volume excitation of the inter-electrode volume was not obtained at pulser power levels less than about 300 W; since the discharge tended to shrink axially towards the hotter gas flow end of the electrode system. This undesirable operational feature was subsequently corrected by adjustment of the fluid ballasting gap of the individual cathode buttons; so as to provide a slight axial grading.

The minor modification not only permitted full volume discharge operation at any level of external pulser ionization, but in addition provided significant improvement in the instability threshold. These aspects are illustrated in Fig. 7; which shows the maximum stable input power plotted as a function of pulser power. Discharge performance is seen to improve markedly even at a low pulser power density. However, at higher pulser power levels, the maximum dc input power reaches a saturation level.

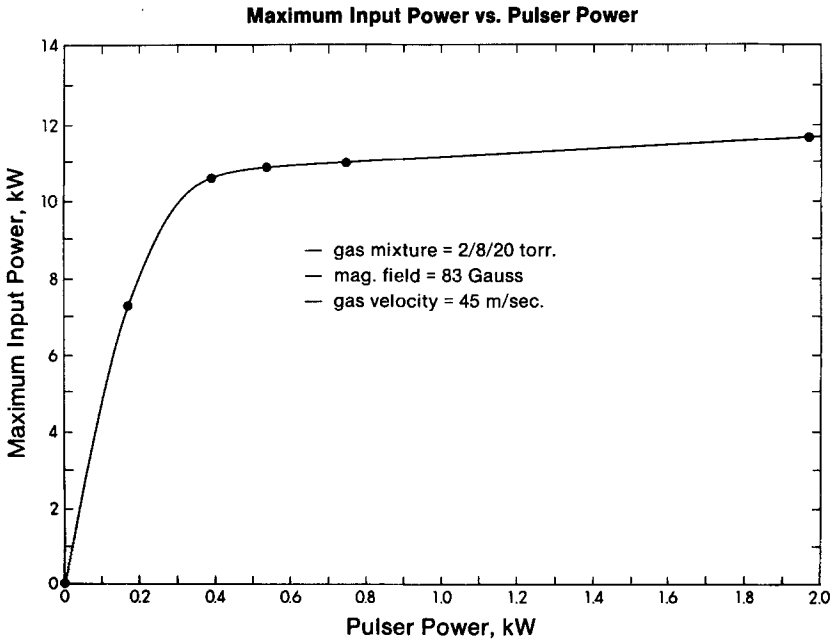

Fig. 7. Maximum input power vs. pulser power

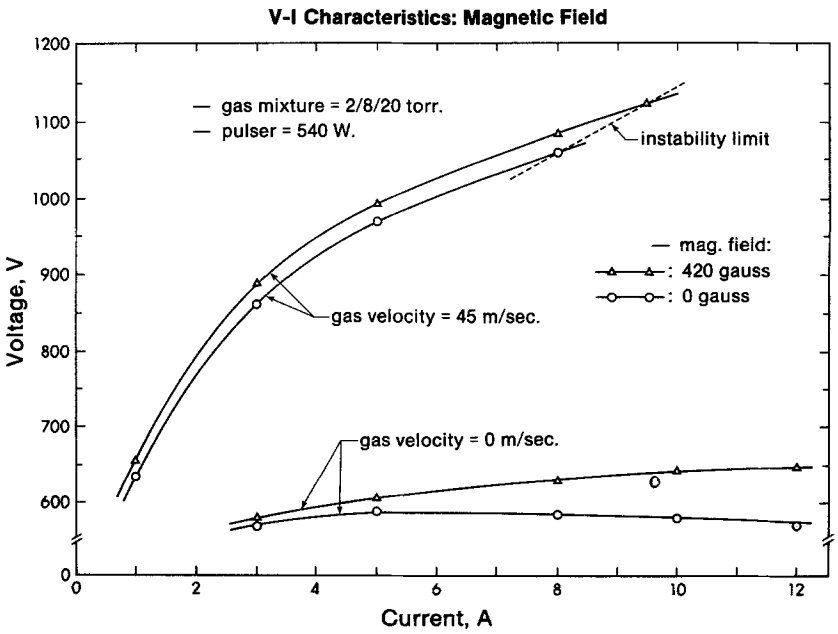

Fig. 8. V–I characteristic: magnetic field

The effect of the applied magnetic field strength on the externally cooled discharge is documented in Fig. 8. Two sets of curves are plotted, one with gas flow and one without. The magnetic field is seen to have a smaller influence on the discharge operating voltage when the gas is convectively cooled. Again, this is due to the increased density of the cooler gas.

The diminished effect of the magnetic field on plasma impedance, when the gas density is increased by convective flow, may be described in the following manner. The electron Hall parameter is given by [20]

$$\beta_e = \omega_e / \nu_{en}, \tag{1}$$

where ω_e is the electron cyclotron frequency and ν_{en} is the electron-neutral collision frequency. It may be shown that β_e can be expressed as

$$\beta_e = eBkT/(m_e V_e Q_{en} P), \tag{2}$$

where B is the magnetic field strength, e is the electronic charge, T is the neutral gas translational temperature, V_e is the mean electron thermal velocity, Q_{en} is the electron-neutral collision cross section, and P is the neutral gas pressure. The Hall parameter is thus directly proportional to both the magnetic field strength and the plasma temperature. Consequently, the relative effect of the magnetic field on the plasma may be expected to diminish as the gas temperature is decreased by convective gas flow.

The magnitude of the Hall parameter may be determined by using typical experimental data. The total gas pressure is 30 Torr, while the average translational temperature of the convectively cooled plasma may be assumed to be about 350 K. The maximum magnetic field strength is 420 G. The electron energy is assumed to be about 1.3 eV, while the collision cross section for the 2/8/20 gas mixture is $Q_{en} = 8.2 \times 10^{-20}$ m^2 [21]. With these parameters, the electron Hall parameter for the convectively-cooled discharge is determined to be approximately $\beta_e = 0.13$.

This value of β_e applies to the convectively-cooled discharge. On the other hand, the plasma temperature will rise to about 700 K when external gas flow is absent. From (4) it is seen that β_e will now have a value of 0.26 (twice its convectively-cooled value), under these higher temperature conditions.

The conductivity of a plasma, under the influence of a magnetic field, in the direction of the applied electric field is given by

$$\sigma_{em} = \sigma_e/(1+\beta_e^2), \tag{3}$$

where σ_e is the electron electrical conductivity in the absence of a magnetic field, and which can be expressed as

$$\sigma_e = n_e e^2 kT/(m_e V_e Q_{en} P). \tag{4}$$

In this expression, n_e is the electron density.

In addition, Ohm's law can be used to relate the applied radial electric field to the radial current density by

$$J_r = \sigma_e E_r. \tag{5}$$

By substituting (3) into (5), the electric field required to maintain a given current density in a magnetized plasma becomes

$$E_r = (1+\beta_e^2) E_{ro}, \tag{6}$$

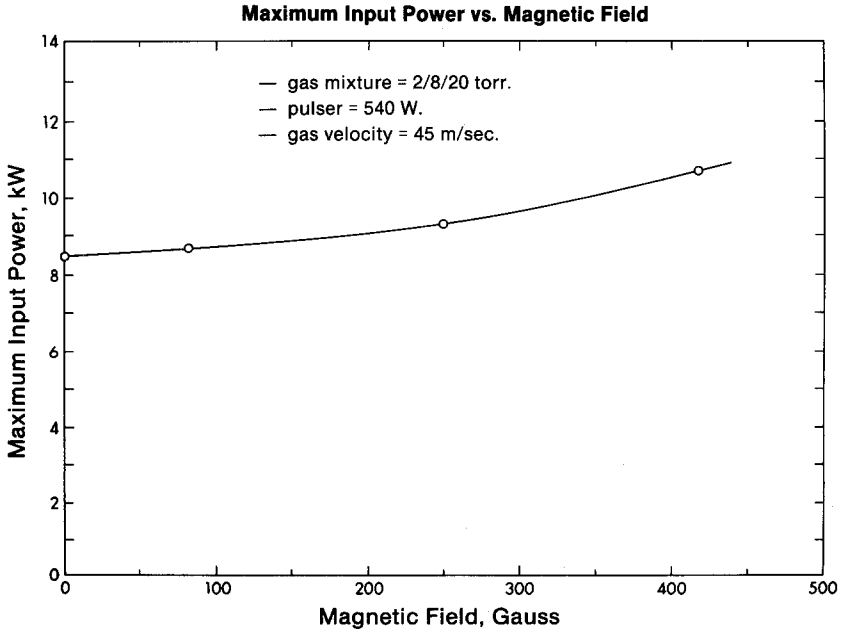

Fig. 9. Maximum input power vs. magnetic field

where E_{ro} is the electric field required when the magnetic field is not applied.

This last expression clearly demonstrates that the magnetic field will have a smaller effect on the terminal characteristics of the discharge when the gas is externally cooled, since the value of β_e is considerably smaller. With convective cooling, the value of β_e was shown to be typically 0.13. The multiplier $(1+\beta_e^2)$ thus has a value of 1.02. With no gas flow, β_e is about 0.26, and thus the multiplier is 1.07. In Fig. 8, the increase in the required discharge voltage is about 25 V out of 1000 V, or about 2.5%, with gas flow. Similarly, the voltage increase is about 45 V out of 600 V, or about 7.5%, without gas flow. Thus, the experimental data is in good agreement with the expected results.

The stabilizing effect of the magnetic field has been previously demonstrated for the case of a non-flow discharge system [13]. The data, illustrated in Fig. 9, confirms that instabilities are also suppressed by the field when external gas flow is present. The maximum dc input power, before the onset of instabilities, is seen to increase by about 25%, as the magnetic field is increased from zero to its maximum strength of 420 G. Clearly, the discharge stabilization mechanism is still quite effective in the convectively-cooled MAGPIE device; despite the low value of β_e obtained with the present system.

3. Discharge Radial Voltage Profile

The glow discharges within gas lasers are comprised of three principle regions [22]. The positive column, which is essentially charge-neutral, physically occupies most of the interelectrode volume. In addition, two very thin (<1 mm) space-charge layers, the cathode and anode fall regions, are located immediately adjacent to the electrode surfaces. Since it is the positive column alone which interacts with the resonant laser mode, only that portion of the dc input power which is actually deposited in this region is available for vibrational excitation. The energy dissipated in both of the thin cathode and anode fall regions is essentially waste heat; which either diffuses to the water cooled electrode surfaces or is convected away by the external gas flow. Consequently, the relative magnitudes of these energy inputs is an important factor in the overall efficiency of the laser device.

To obtain this data, several measurements were made of the floating potentials within the gas discharge, using both scanning and stationary voltage probes. First, several plasma voltage profiles were obtained across the interelectrode gap, as illustrated in Fig. 10. Each curve represents operation at a different pulser power level. For illustrative purposes, the physical widths of the cathode and anode fall regions have been exaggerated in this plot. The main feature to be observed here is that the voltage is not linear, which implies that the electric field (dV/dr) is not constant. This is in sharp contrast to the constant field profiles usually assumed for both axial and transverse gas discharges [22].

In order to examine this aspect further, the radial electric field profile is plotted in Fig. 11, for two different pulser power levels. In both cases, the field is

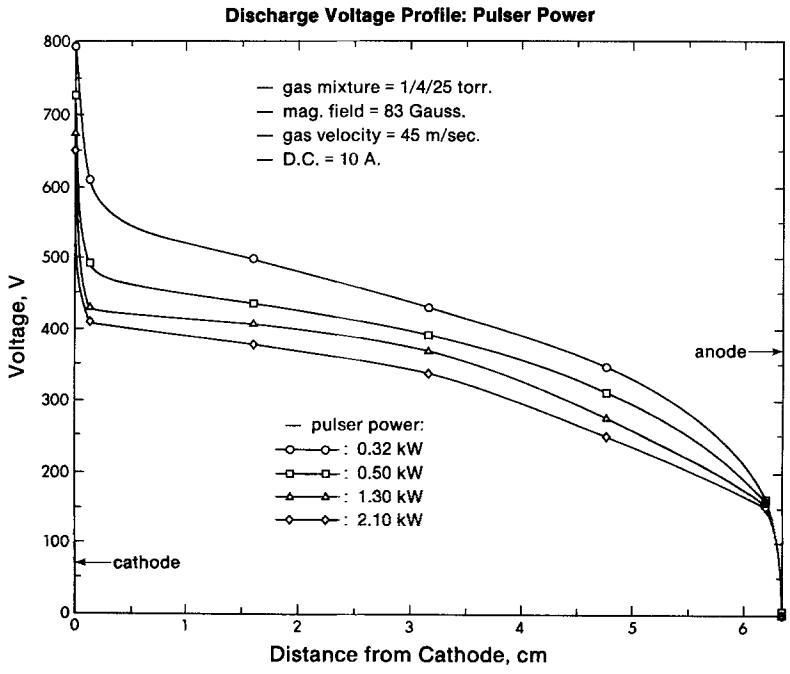

Fig. 10. Discharge voltage profile: pulser power

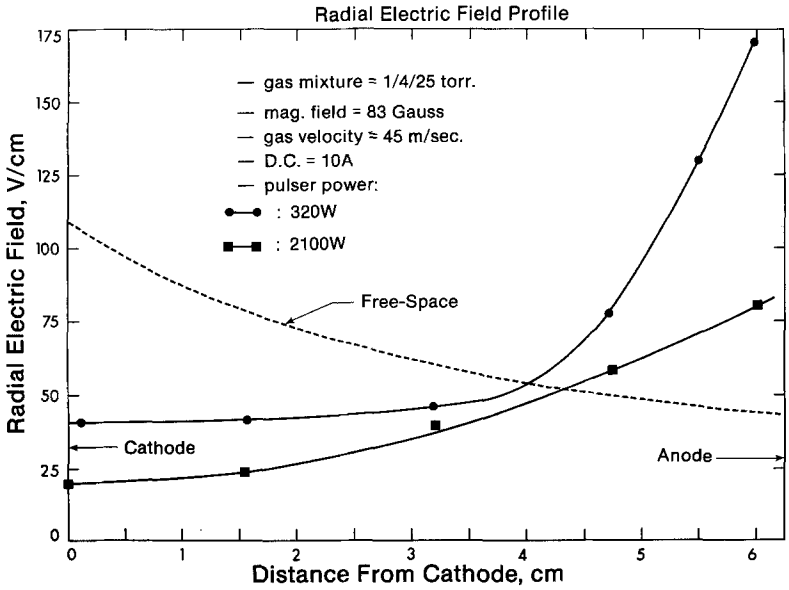

Fig. 11. Radial electric field profile

observed to be low and relatively constant near the center cathode, but increases markedly near the outer anode. Also, both the absolute value of the field and the degree of radial variation are reduced as the pulser power is increased. When the degree of preionization is relatively small (near self-sustained), the field near the cathode is about 40 V/cm; while near the anode it is about 170 V/cm; a factor of four greater.

The observation that the electric field in the positive column is highest at the outermost electrode is particularly interesting. In the absence of the plasma, the radial electric field variation would be expected to be that of a simple coaxial capacitor; namely [10]:

$$E(r)=V_0/[r\ln(b/a)]\,, \tag{7}$$

where V_0 is the applied voltage between the coaxial electrodes, and a and b are the inner and outer radii, respectively. Equation (7) indicates that, in the absence of a discharge, the highest electric field would be at the inner cathode surface. The substantial difference between the observed field profiles and the coaxial capacitor (free-space) variation is clearly evident in Fig. 11, where the free-space ($1/r$) field profile is shown as a dashed line.

The unusual electric field profile observed in the coaxial discharge may best be rationalized in terms of a radial variation in the electron density. This may be deduced from the following considerations. The total radial current density within the discharge can be expressed as the sum of the electron, negative ion, and positive ion currents

$$J_r=e(n_p\mu_p-n_e\mu_e-n_n\mu_n)E_r\,, \tag{8}$$

where n_p, n_e, and n_n are the positive ion, electron, and negative ion densities; and μ_p, μ_e, and μ_n are the positive ion, electron, and negative ion mobilities. Since the positive column is essentially charge-neutral, $n_p=n_e+n_n$. Also, the electron mass is much smaller than the ion masses, and therefore $\mu_e\gg\mu_n$, μ_p.

Consequently, the total current density is essentially that of the electrons, the ion contributions being small in comparison. Therefore

$$J_r\sim J_e=-en_e\mu_eE_r\,. \tag{9}$$

This may also be expressed as

$$J_r(r)=I/(2\pi L_D r)=-en_e(r)\mu_e(r)E_r(r)\,, \tag{10}$$

where I is the total discharge current and L_D is the discharge axial length.

As mentioned previously, the axial gas velocity in the MAGPIE system is uniform in radius, which is characteristic of highly turbulent flow. This implies that there is a considerable amount of gas mixing in the radial direction, which would tend to make the plasma isothermal. Consequently, in the following discussion, the electron mobility μ_e may be assumed to be constant in the radial direction.

With the assumption of constant electron mobility, (10) may be rearranged to give the following expression for the electron density

$$n_e(r)=I/[2\pi L_D e\mu_e rE_r(r)]\,. \tag{11}$$

If the electron density is assumed to be uniform throughout the discharge (no radial dependence), then the resulting electric field is determined as follows

$$n_e(r)=\text{const}=I/[2\pi L_D e\mu_e rE_r(r)]\,, \tag{12}$$

or in terms of E

$$E_r(r) = \text{const}/r . \tag{13}$$

It follows from this, that if there is no radial variation in electron density, the discharge will exhibit a free-space electric field profile. This result is consistent with observations in axial tube discharges [22], where both $n_e(x)$ and $E_x(x)$ are constant. However, since the electric field in the MAGPIE discharge does not in fact exhibit a free-space (l/r) variation, it must be concluded that $n_e(r)$ is not constant.

As a first approximation, the actual electric field depicted in Fig. 11 may be expressed as an exponential, or $E_r(r) = Ce^r$. If this expression is substituted into (11), the result is

$$n_e(r) = I/(2\pi L_D e \mu_e r C e^r) = (C'/r)e^{-r} . \tag{14}$$

Thus, in the discharge under study, the electron density appears to be decreasing exponentially with radius.

The precise reason for this exponential decrease in electron density is not entirely clear at this time, and is currently the subject of additional study. However, these results, along with other recent data obtained from a PIE transverse discharge system, suggest that electron attachment to CO_2 molecules may be largely responsible. It is suspected that electrons emitted from the center cathode are continuously being lost through attachment, and thus their density decreases with increasing radius. Since the external pulser ionization source produces additional electrons uniformly throughout the discharge volume, the variations in both electron density and electric field are expected to be less dramatic when a large degree of external preionization is employed.

4. Discharge Potential Measurements

Measurements were also made of the voltage drops across the three principle discharge regions (positive column, cathode fall, and anode fall) as various parameters were varied. The first of these plots, shown in Fig. 12, reveals the manner in which these voltages vary with discharge current. All three potentials are seen to rise as the current increases. This behavior is reasonable since an increasing number of electrons must be transported across the interelectrode gap. The positive column voltage is also seen to level off to a steady-state value beyond a current of 5 A. This is consistent with a constant-voltage behavior characteristic of a normal glow discharge.

The plot of Fig. 12 also demonstrates that relatively large power losses occur in the cathode and anode fall regions. For example, at a total current of 8 A the positive column voltage drop is 460 V, while the combined cathode and anode voltage drop is 530 V. Thus, only 46% of the total discharge input power is actually available for vibrational pumping.

This relatively poor electrical efficiency is also evident in a number of transverse discharge lasers, which also feature a small interelectrode spacing. Axial discharge devices, on the other hand, are generally more efficient as a result of their much larger electrode separation. This is due to the fact that the positive column voltage increases with electrode spacing, while the cathode and anode falls remain essentially constant.

The curves of Fig. 13 reveal the variation of these plasma potentials as a function of gas flow velocity. In this case the anode fall remains relatively unchanged,

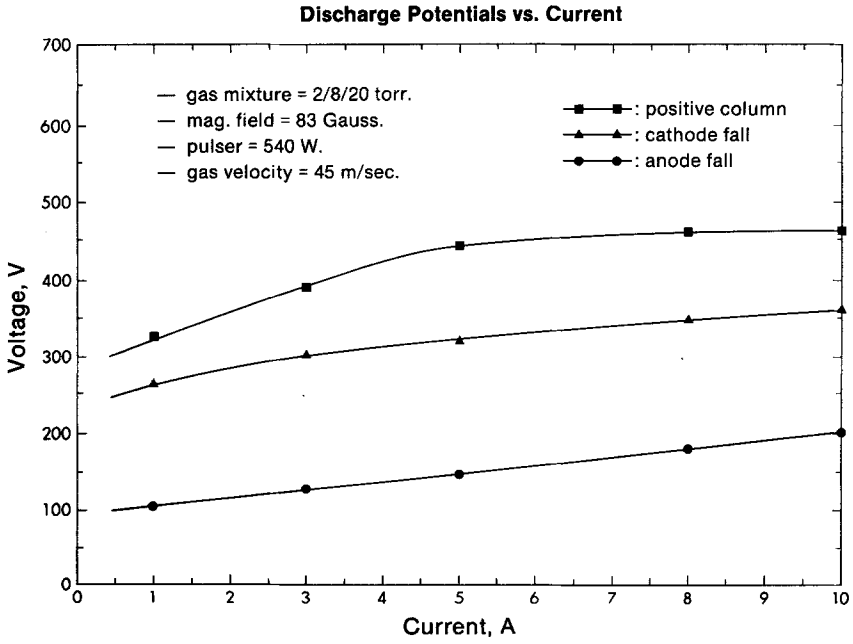

Fig. 12. Discharge potentials vs. current

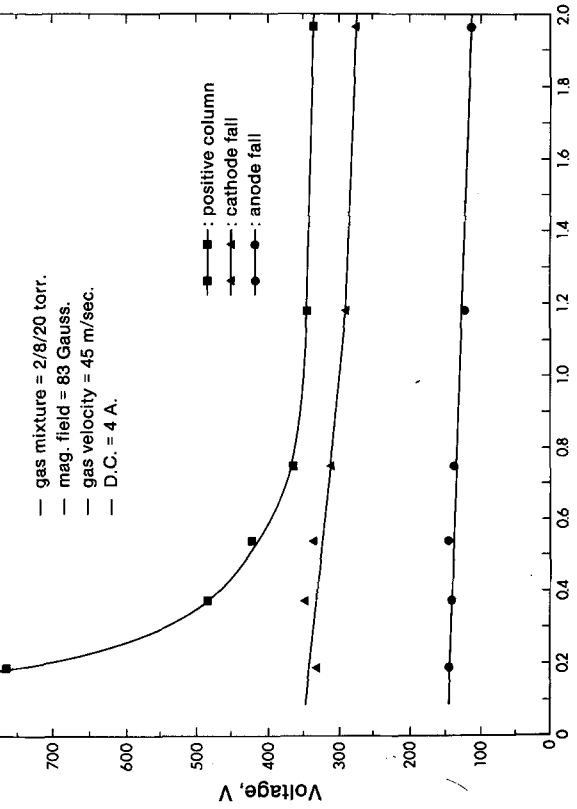

Fig. 14. Discharge potentials vs. pulser power

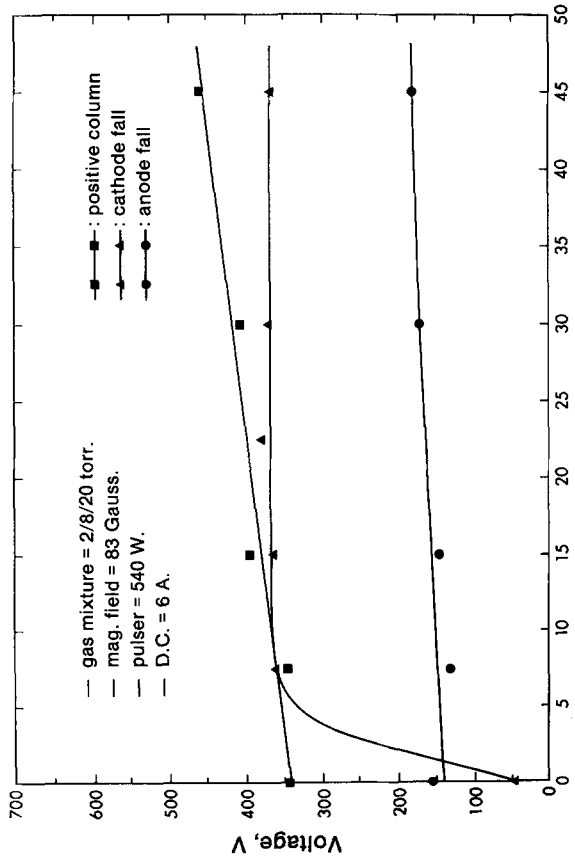

Fig. 13. Discharge potentials vs. gas velocity

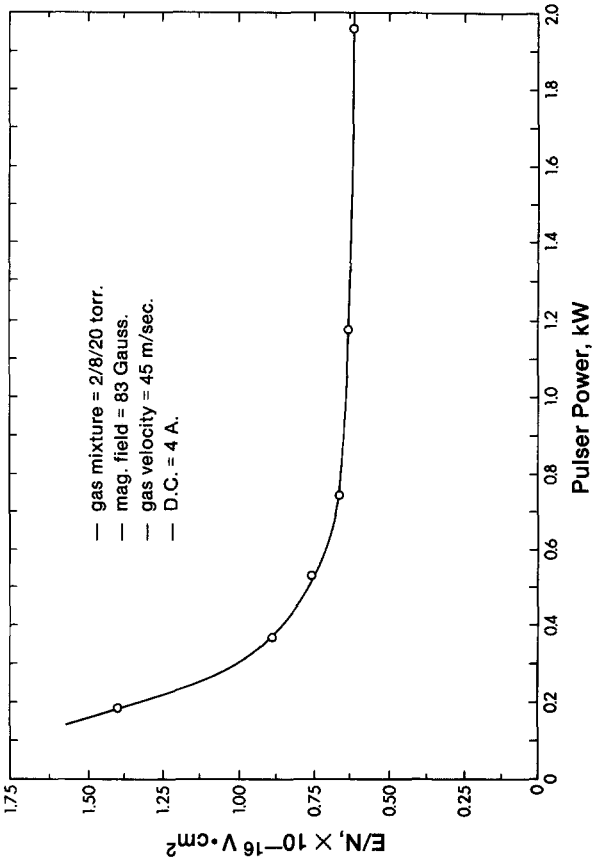

Fig. 16. E/N vs. pulser power

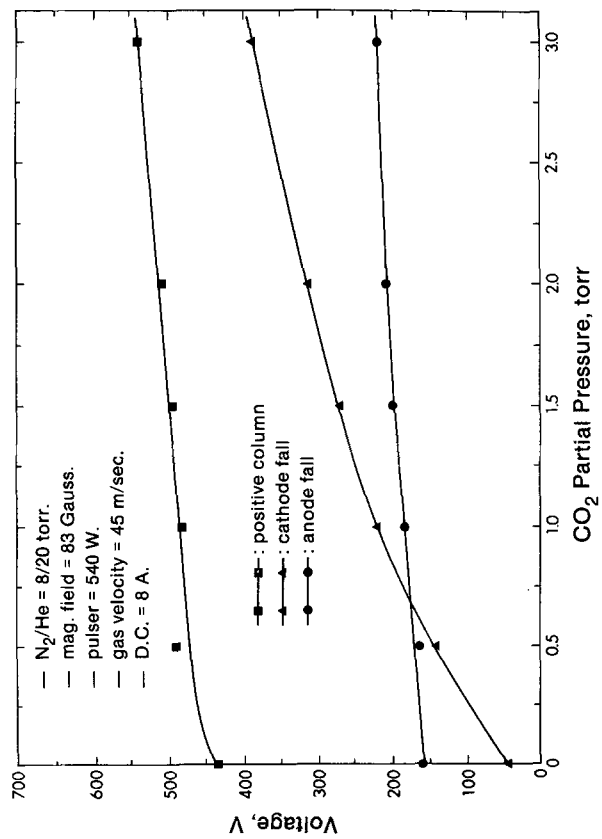

Fig. 15. Discharge potentials vs. CO_2 partial pressure

since the discharge current is kept constant. However, the cathode fall behavior is considerably more interesting. With no gas flow, V_{cf} is only about 50 V. However, as the gas velocity is increased, V_{cf} rises rapidly to about 350 V; seven times its non-flow value. It then levels off at this constant value for velocities greater than about 7 m/s.

The phenomena described above is not yet fully understood. However, it is likely that temperature effects are again involved. In the absence of external gas flow, heat can only be removed from the cathode fall region by thermal diffusion to the water-cooled cathode surface. Thus, the temperature of the cathode fall region may become quite high, resulting in an increased mobility of the ions that bombard the cathode surface. Thus, only a small cathode fall electric field would be required to liberate electrons via secondary emission.

However, even a small amount of turbulent convective flow can cool the cathode fall region, thus significantly reducing ionic mobility. This effect would in turn be reflected in a large increase in the cathode fall voltage that is required to maintain the same rate of secondary electron emission.

The factor which most influences the positive column voltage is the level of external pulser ionization. This feature is well illustrated in Fig. 14. The positive column voltage is seen to remain essentially constant at pulser power levels above 1 kW; corresponding to a pulser power density of 100 W/l. Below this value, however, the voltage increases rapidly, as the discharge approaches a self-sustained operating condition.

Another intriguing result was obtained when the carbon dioxide partial pressure was varied. This phenomena is illustrated in Fig. 15. As expected, all three voltages rose with increasing CO_2 concentration. However, the cathode fall variation observed was particularly dramatic. In fact, the cathode fall almost completely disappeared (50 V) when there was no CO_2 in the gas mixture.

This effect is quite similar to that shown in Fig. 13. In this case, however, the gas flow velocity, and thus the ion mobility in the cathode fall region, is constant. Consequently, it must be concluded that CO_2 attachment effects are responsible for this large change. It is likely that the electrons emitted from the cathode are rapidly lost through attachment, when CO_2 is present. Such a condition would require an increase in the rate of secondary emission by ion bombardment of the cathode surface, in order to maintain a constant current. The net result would therefore be a large increase in the cathode fall voltage required to accelerate the ions to sufficient energy for secondary emission.

Previous theoretical work by Lowke et al. [23] has shown that the value of the electric field/molecular density ratio, or E/N, is important in determining the efficiency of vibrational excitation within a CO_2 laser gas discharge. Consequently, this parameter has been calculated from the positive column voltage drop presented earlier. As expected, a very pronounced effect on E/N is observed when the pulser power is varied. This influence is illustrated in Fig. 16. At a constant discharge current, E/N is observed to increase markedly as the pulser power is reduced below about 400 W. However, the discharge stability limit is observed to decrease simultaneously. For the 30 torr gas mixture normally used in these tests, a pulser power level of about 300 W yielded an E/N of about 1.0×10^{-16} V cm^2, which is nearly optimum for vibrational excitation of the (001) upper laser level of the CO_2 molecule.

5. Conclusion

The experimental results described above demonstrate the successful operation of the convectively cooled MAGPIE coaxial discharge system. Interestingly the relatively weak magnetic fields used had only a small effect on the discharge terminal characteristics, despite their well demonstrated stabilizing influence on the plasma itself. The important E/N ratio was calculated to be about 1.0×10^{-16} V cm^2. This value is essentially optimum for efficient vibrational excitation of the CO_2 laser transition. These results indicate that there is considerable potential for obtaining efficient laser performance in such a device. Finally, in-situ voltage measurements indicate that CO_2 attachment effects have a considerable influence on the operation of this type of laser gas discharge.

Recently, small-signal gain and laser power extraction measurements have also been performed, using this novel MAGPIE coaxial discharge system. The results of these studies will be published in due course.

Acknowledgement. The authors gratefully acknowledge the continuing financial support of the Natural Sciences and Engineering Research Council of Canada.

References

1. C.J. Buczek, R.J. Wayne, P.P. Chenausky, R.J. Frieberg: Appl. Phys. Lett. **16**, 321 (1970)
2. C.J. Buczek, R.J. Freiberg, P.P. Chenausky, R.J. Wayne: Proc. IEEE **59**, 659 (1970)
3. M. Yessik, J.A. Macken: J. Appl. Phys. **54**, 1693 (1983)
4. S. Ono, S. Teii: Rev. Sci. Instrum. **54**, 1451 (1983)
5. H.J.J. Seguin, C.E. Capjack, D.M. Antoniuk, K.H. Nam: Appl. Phys. Lett. **37**, 130–132 (1980)

6. C.E. Capjack, D.M. Antoniuk, H.J.J. Seguin: J. Appl. Phys. **52**, 4517–4525 (1981)
7. R.K. Garnsworthy, L.E.S. Mathias, C.H.H. Carmicheal: Appl. Phys. Lett. **19**, 506 (1971)
8. L.W. Casperson, M.S. Shekhani: Appl. Opt. **14**, 2653 (1975)
9. G.R. Osche, H.E. Sonntag: IEEE J. QE-**12**, 752 (1976)
10. K.T.K. Cheng, L.W. Casperson: Appl. Opt. **18**, 2130 (1979)
11. H.J.J. Seguin, C.E. Capjack, D.M. Antoniuk, V.A. Seguin: Appl. Phys. Lett. **39**, 203–206 (1981)
12. C.E. Capjack, H.J.J. Seguin, D.M. Antoniuk, V.A. Seguin: Appl. Phys. B **26**, 161–170 (1981)
13. V.A. Seguin, H.J.J. Seguin, C.E. Capjack: Appl. Opt. **24**, 1265–73 (1981)
14. V.A. Seguin, H.J.J. Seguin, C.E. Capjack: Rev. Sci. Instrum. **55**, 1445–1455 (1984)
15. K.H. Nam, H.J.J. Seguin, J. Tulip: IEEE J. QE-**15**, 44 (1979)
16. V.E. Merchant, H.J.J. Seguin, J. Dow: Rev. Sci. Instrum. **49**, 1631 (1978)
17. N. Tabata, H. Nagai, H. Yoshida, M. Hishii, M. Tanaka, Y. Myoi, T. Akiba: 5th. Gas Flow and Chemical Lasers Symposium, Oxford, U.K. (1984)
18. Li. Zaiguang, Li. Jiarong, Cheng Zuhai, Chen Quinmin, Zhang Yongfang, He Xuhui: 5th Gas Flow and Chemical Lasers Symposium, Oxford, U.K. (1984)
19. W.L. Nighan, W.J. Wiegand: Appl. Phys. Lett. **25**, 633–635 (1974)
20. M. Mitchner, C.H. Kruger, Jr.: *Partially Ionized Gases* (Wiley, New York 1973) pp. 177–185
21. D.M. Antoniuk: "A Magnetogasdynamic Approach to Laser Discharge Stabilization", Ph.D. Thesis, University of Alberta (1983) pp. 84–90
22. E. Nasser: *Fundamentals of Gaseous Ionization and Plasma Electronics* (Wiley, New York 1971) pp. 398–412
23. J.J. Lowke, A.V. Phelps, B.W. Irwin: J. Appl. Phys. **44**, 4664–4672 (1973)

Responsible for Advertisements: E. Lückermann, G. Probst, Heidelberger Platz 3, D-1000 Berlin 33, Tel. (030) 8207-1, Telex 01-85411
Responsible for the Text: H. K.V. Lotsch, Tiergartenstrasse 17, D-6900 Heidelberg. Printers: Brühlsche Universitätsdruckerei, Giessen

Springer-Verlag GmbH & Co. KG, D-1000 Berlin 33